RIN: Textured Human Model Recovery and Imitation with a Single Image

Haoxi Ran¹*, Guangfu Wang², Li Lu¹
¹Sichuan University, ²Megvii Technology

ranhaoxi@gmail.com
wangguangfu@megvii.com
luli@scu.edu.cn

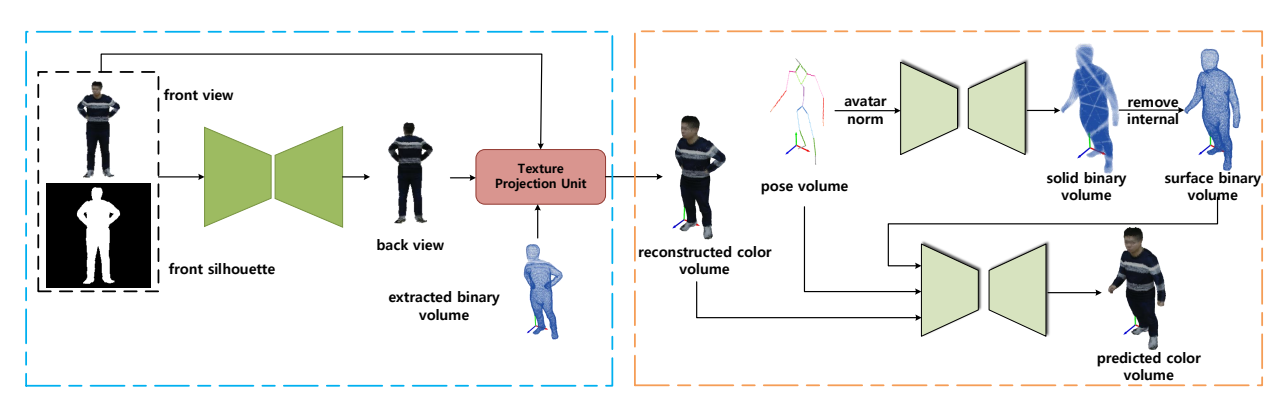


Figure 1. An overview of our framework. Our framework contains two parts, one is to recovery a fully-textured human body and the other is to imitate human action. The human recovery module will first estimate the back-view image from the front image and its silhouette. The Texture Projection unit then recovers the human body with the two images. The human imitation module contains two streams. One is to generate binary volume from the given pose, or pose-to-binary-volume translation. The other is to imagine the textured human body with the generated binary geometry and its pose.

Abstract

Human imitation has become topical recently, driven by GAN's ability to disentangle human pose and body content. However, the latest methods hardly focus on 3D information, and to avoid self-occlusion, a massive amount of input images are needed. In this paper, we propose RIN, a novel volume-based framework for reconstructing a textured 3D model from a single picture and imitating a subject with the generated model. Specifically, to estimate most of the human texture, we propose a U-Net-like front-to-back translation network. With both front and back images input, the textured volume recovery module allows us to color a volumetric human. A sequence of 3D poses then guides the colored volume via Flowable Disentangle Networks as a volume-to-volume translation task. To project volumes

to a 2D plane during training, we design a differentiable depth-aware renderer. Our experiments demonstrate that our volume-based model is adequate for human imitation, and the back view can be estimated reliably using our network. While prior works based on either 2D pose or semantic map often fail for the unstable appearance of a human, our framework can still produce concrete results, which are competitive to those imagined from multi-view input.

1. Introduction

The capability of human imitation with a fully textured geometric model from a single image can open the door to countless applications, such as virtual and augmented reality, virtual human animation, gaming and filming. A framework that can generate a sequence of 3D human motion via only one photo exceedingly inspires the production of immersive content creation with virtual humans. How-

^{*}This work is done when Haoxi Ran is a research assistant in Sichuan University.

ever, due to self-occlusion, such a generation process can be arduous with the infinite possibilities of shapes and appearances. Meanwhile, we can only extract limited human features from a 2D projection in the real world.

In recent years, generative adversarial network (GAN) [10] has shown remarkable success in synthesizing unseen images and disentangling the pose or correspondence map and content [19, 20, 31, 13]. Prior approaches mainly rely on the 2D poses and semantic maps, keeping the generation process in 2D space. Thus, self-occlusion is unavoidable, and massive human features are missing. Accordingly, the methods have poor performance on one frame poseguided transfer. The problem causes white space appearing or twisted human shape since the process heavily relies on a 2D pose label, which is not sensitive to the rigid transformation of human parts in 3D space. The previous approaches cannot present reasonable layout locations to twist human shape from a given personalized one to an unnatural one. To weaken the problem, some recent work [17, 6] takes plenty of multi-view images as input. The appearance is still unstable in practice, especially head. Furthermore, a large amount of input (usually more than 500 frames) leads to high computational costs and impracticability. Besides, recent methods [17, 22] try to recover geometric information and fuse them into pose transfer flow, whereas the methods manipulate motion to transfer based on the SMPL template [18], a parametric human body model. Such a parametric model seems to be a wise choice for its smooth surface as well as a human-like shape. However, the weakness that considerable geometric details (i.e., clothing, wrinkles, irregular head part for long hair, or else) are missing, is uncovered when we apply the methods to a real scene. Subsequently, the results of these methods will lose some features of the original input during learning. In summary, the methods above encounter three main challenges in generating pose-transfer realistic images as follows:

- It is difficult to break through pixel-level space for diverse possibilities to avoid self-occlusion.
- The output appearance of the subject is unstable for the guidance of critical points, dense pose, or semantic segmentation at the image level.
- It is inefficient to fully texture a SMPL model.

In this paper, to utilize geometric information of the human body, we propose Textured Human Model Recovery and Imitation Networks, or RIN, a framework mostly based on generative adversarial network to address the three challenges above. Specifically, to preserve geometric details (including clothing and wrinkles) and to produce a reasonable initialized 3D model, we leverage volumetric humans instead of the SMPL model by feeding input images into

a pretrained DeepHuman framework [35]. To avoid self-occlusion, we texture human models based on volumetric geometry. Through our front-to-back translation network, we first estimate the back-view image with front-view image input. Given the front-view silhouette, we can obtain the back-view silhouette by flipping.

Based on the assumption that the visual elements of front and back views are nearly the same [21], our front-to-back translation network synthesizes the back view from the front one. Provided with the double views, for the convenience to input, we project each pixel to each voxel of volumetric geometry on both sides.

To imitate human action based on 3D space, we feed Pose-Guided Flowable Networks, a volume-to-volume translation CNN, with both the colored volume and source 3D pose. Our networks then enable a sequence of 3D pose labels to guide the textured geometry to perform different action. Note that since each action of the geometric avatar is in 3D space, we use an immobile plane to simulate the real human action.

We evaluate the front-to-back synthesis part on our synthetic body mesh dataset and human imitation on THuman dataset [35]. Our RIN produces comparable human imitation models from a single image with the stability of human appearance and high fidelity of human geometric details. It is competitive with those multi-view input approaches. We believe that in the more immediate future, human imitation from a single view can evoke new waves of VR/AR content creation.

2. Related Work

Human motion imitation. In recent years, human motion imitation has become a popular topic in the generative model. Existing approaches are on the base of either conditional generative adversarial networks [10] or Variational Auto-Encoder [7]. In contrast, CGAN is the preferred choice for its capability of high-quality image generation as well as the tolerance of various labels(i.e., human pose, semantic map, and dense pose). [19] designs a U-Net-like generator utilizing coarse-to-fine manner to generate human images. Similarly, [26, 4] adopt a multistage adversarial losses. Also, they consider synthesizing the human body and inpaint background in parallel. In [6], pix2pixHD networks combined with a Face GAN to enhance the features of human face pursue a high-resolution human image. Furthermore, [17] and [22] have taken geometric information into consideration and fuse SMPL model into their framework. While the first method initializes input with the SMPL model, the other utilizes DensePose [2] to obtain labels. Most of these approaches learn a latent space that maps a pose to a real human image. However, the limitation of such a method is that every avatar is needed to train in their network. In other words, it is not allowed to

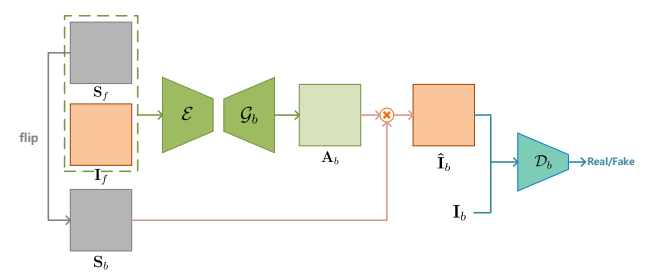


Figure 2. Illustration of our front-to-back synthesis network.

train more than two persons, even the same person with two different kinds of clothing in one network. However, [17] learns a distribution of different avatars by Liquid Warping Block and a U-Net-like generator. Inspired by this technical idea, our Pose-Guided Flowable Networks extract human clothing and wrinkle details by a 3D U-Net on the task of reconstruction.

Single-view reconstruction. In order to reduce the solution space of human geometry, SCAPE [3] and SMPL [18] are introduced for single-view reconstruction. Most singleview reconstruction approaches estimate a model by estimating the parameters of the human model template. In [5, 15, 28, 16, 29, 33], they tries to best match an image for human reconstruction. In [24], the authors utilize hybrid annotations for human recovery, and the framework can handle different scenes for human reconstruction. For the highly non-linear feature of the parametric model, deep learning networks have been popular for parameter estimation. However, the difference between those methods is merely in network architectures, input labels, and loss functions. Although deformable models are tractable for estimation, they cannot be qualified for fine-scale clothing details and geometric wrinkles. Some methods hence incorporate in 2D and 3D pose to assist in preserving the detailed geometric information. In [8, 14, 30], volumetric human models or point clouds are heavily relied on for preserving geometric details. Both [35] and [8] recover the human model from a volume with the help of the SMPL model. Moreover, additional labels play an important role in other methods. [21] introduces a silhouette-based representation for human recovery, and [1] makes full use of 2D dense pose for model recovery. Inspired by [35], we propose to achieve the task of human imitation based on a volumetric model.

3. Method

Our RIN(Texture **R**ecovery and Imitation **N**etworks) includes three modules, front-to-back texture synthesis (Sec. 3.1), textured human recovery based on volume (Sec. 3.2) and pose-guided human animation with our Flowable Networks (Sec. 3.3). Fig. 1 illustrates the overview of our pipeline. Given a frontal image as input, denoted by \mathbf{I}_f , we aim to reconstruct a complete textured human

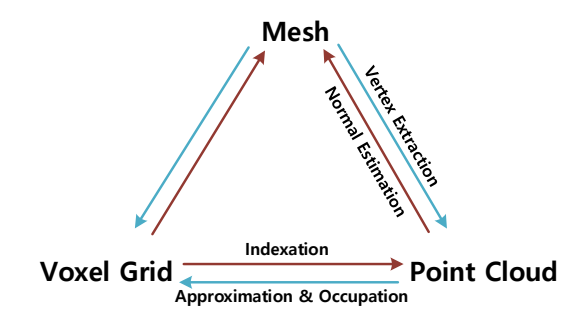


Figure 3. Three most popular representation applied in deep learning. One of them can convert to another type directly or indirectly.

model and then to imitate action from a source video with this model. We base our method on the volumetric model for the incompatibility of fitting real-world humans by the SMPL model. With volumetric models, we can preserve the clothing details as well as its wrinkles. However, due to self-occlusion and possible inconsistency between the front and back views, recovering a full textured human model is most challenging. To further improve the quality of the output, we adopt a front-to-back synthesis method similar to SiCloPe [21] to estimate the back view corresponding to the input image. We subsequently reconstruct the textured human model at the voxel level. Finally, we guide the model in a deep learning manner via a sequence of poses without the need of human manipulation.

We first extract the silhouette \mathbf{S}_f as well as the 3D pose \mathbf{P}_s , estimated from the given image \mathbf{I}_f . Provided with \mathbf{I}_f , our front-to-back synthesis network will estimate the back view $\hat{\mathbf{I}}_b$ with the assistance of \mathbf{S}_f . We then exploit state-of-the-art method DeepHuman [35] to obtain binary volume \mathbf{B}_s from \mathbf{I}_f . Our texture recovery module will reconstruct the colored volumetric model \mathbf{C}_s from \mathbf{I}_f and $\hat{\mathbf{I}}_b$ based on \mathbf{B}_s . Finally, to imitate the source video, we extract a sequence of 3D poses via a triangulation method [12] and then guide \mathbf{C}_s by one target pose \mathbf{P}_t , with a result of \mathbf{C}_t .

3.1. Front-to-Back Synthesis

Due to self-occlusion, directly recovering a full-textured human model is challenging. Therefore, we convert this tough question into a relatively simple task by estimating the back view related to the input and inpainting both images on the voxel grid. We uncovered that both views share the same contour. Thus just flipping can get the ground-truth silhouette of the back view. This observation inspired us to deal with such a problem as an image-to-image translation. Additionally, to prevent the possibility of out-of-boundary condition, our networks take \mathbf{S}_f as an attentional map and apply it to the synthesized image prior to supervision, which presents its excellence shown in Fig. 8. In

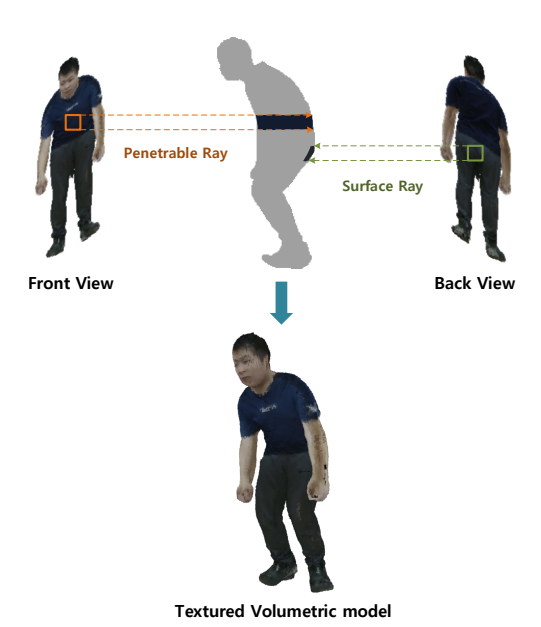


Figure 4. Illustration of our texture projection unit.

order to solve the problem of GAN's instability to estimate unseen scenes caused by occlusion, we propose a front-to-back translation model (shown in Fig. 2).

As shown in Fig. 2, given the frontal image \mathbf{I}_f with a white background, we first extract the image into a binary mask \mathbf{S}_f , where the white pixels are set to 0, and the others are 1. If an in-the-wild image is needed to handle, we need to extract its silhouette via an instance segmentation tool. We train on the encoder \mathcal{E} and the generator \mathcal{G}_b to generate $\hat{\mathbf{A}}_b$ and $\hat{\mathbf{S}}_b$, with the supervision of ground truth back view \mathbf{I}_b as well as the flipped silhouette \mathbf{S}_b . The output avatar can be obtained as follows:

$$\hat{\mathbf{A}}_b = \mathcal{G}_b \left(\mathcal{E} \left(\mathbf{S}_f, \mathbf{I}_f \right) \right).$$

To prevent blurry boundary of outputs as well as to constraint content within silhouettes, we apply mask S_f to the avatars before supervision:

$$\hat{\mathbf{I}}_b = \hat{\mathbf{A}}_b \odot \mathbf{S}_b + 1 \odot (1 - \mathbf{S}_b),$$

where \odot represents Hadamard product. Specifically, our networks are supervised by two patch-based discriminators \mathcal{D}_f and \mathcal{D}_b with respect to generators \mathcal{G}_f and \mathcal{G}_b .

3.2. Textured Human Model Reconstruction

We have various choices of geometry representations for deep learning frameworks, shown in Fig. 3. Specifically, mesh is much common in graphics for its convenience. Point cloud contains points to express the exact location directly. However, a deep learning framework cannot easily understand both of them for their specific ways to represent a model. Voxel grid, in contrast, is popular for its simple structure and compatibility of volumetric convolution,

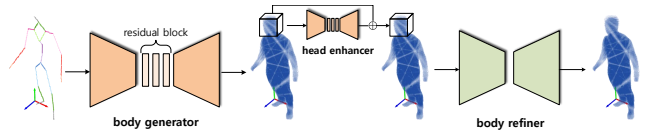


Figure 5. Illustration of our pose-to-binary translation network.

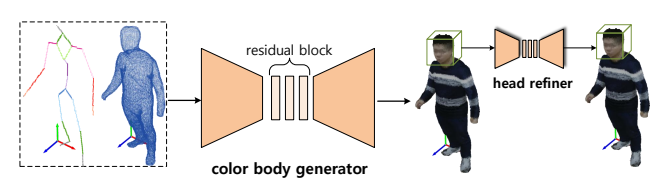


Figure 6. Illustration of our binary-to-color translation network.

which means the voxel grid can be both the input and the output of a framework without preprocessing. To seek an effective method to represent the model, we adopt the voxel grid.

To freely convert each representation to another, we need to survey the three structures. In order to obtain the voxel grid from a point cloud, we seek to approximate a set of points to integer indices and occupy voxels with these indices. Each approximated index keeps the original RGB information. We call this process Approximation & Occupation. The inverse process of such a convert is Indexation, deriving each point location from the voxel index. Although obtaining mesh from a point cloud is tough, some existing tools (i.e., open3D [36]) can assist us in getting the corresponding mesh from a point cloud. However, the vertices of a mesh can directly be a point cloud, sometimes needed to be densified. The voxel grid takes the point cloud as a middleware to generate a mesh and vice versa.

Inspired by the front-to-back rendering method [21] to reconstruct the texture of a mesh, we propose a novel method to recover a textured volume. As is shown in Fig. 4, given front-view and back-view images, we project each pixel of the frontal image to the voxels along with the penetrable ray. The voxels contain not only the surface voxels but the occluded voxels. We then project the back-view image to the back-view surface of the volume. Our penetrable ray can handle the voxel-wise occlusion, as well as preserving its natural appearance, which can fully overcome the color inconsistency problem from volumetric front-to-back rendering. The surface ray preserves the visible features of the back-view image. Novel view synthesis can, at the same time, be an appropriate manner to evaluate the effectiveness of our reconstruction module compared with other methods [17, 23].

3.3. Pose-Guided Flowable Networks

In this part, we propose a novel network to guide a volumetric model with a sequence of poses. Although some existing methods [19, 6, 4] succeed in generating unseen

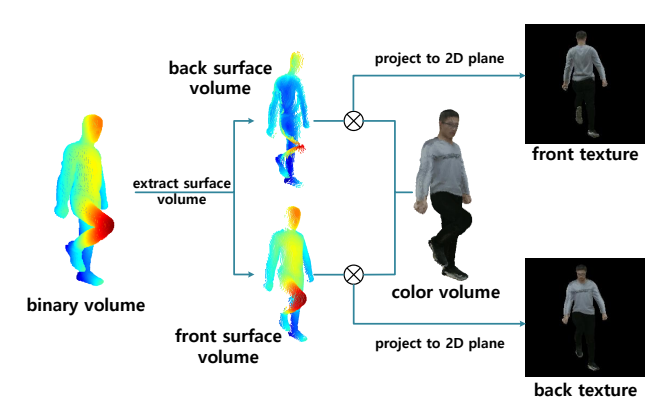


Figure 7. Illustration of our depth-aware differentiable renderer for volumes.

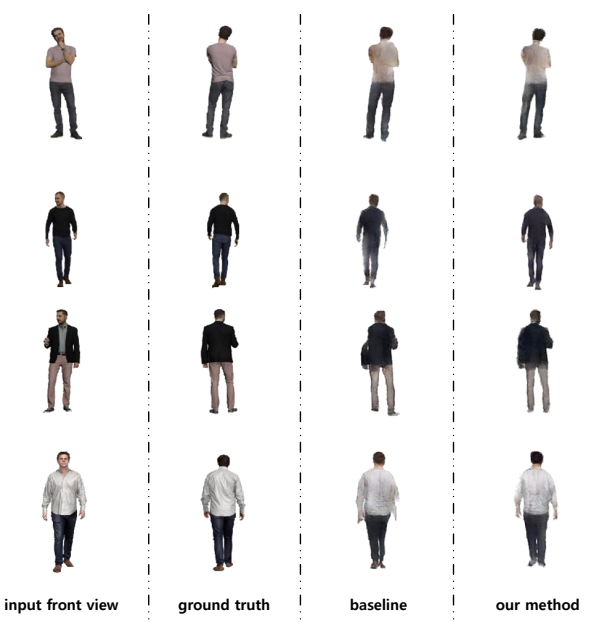


Figure 8. Comparison of our method with the baseline model from SiCloPe[21] on our synthetic dataset. We apply pre-flip and silhouette-based attention map to our front-to-back synthesis network. These tricks help keep the total shape of a person and improve the quality of the image as well. Additionally we can directly apply the output back-view image to our texture projection unit without losing information.

poses at the image level, guiding a volumetric human is much challenging for the sparsity of a volume. As shown in Fig. 6, our framework, therefore, synthesizes a binary volume before gaining the final colored volume.

Our proposed Pose-guided Flowable Networks works in a two-stream manner. One stream contains a pose-to-binary-volume generator \mathcal{G}_{p2b} as well as a binary-volume-to-pose generator \mathcal{G}_{b2p} . Provided with a volumetric pose \mathbf{P} , \mathcal{G}_{p2b} works on synthesizing the solid binary volume $\hat{\mathbf{B}}$:

$$\hat{\mathbf{B}} = \mathcal{G}_{n2b}\left(\mathbf{P}\right)$$
.

We allow \mathcal{G}_{p2b} to generate a solid volume in order to reduce the sparsity of a volume and thus easily extract the geometric shape. We train \mathcal{G}_{b2p} together with \mathcal{G}_{p2b} to supervise through the prior input \mathbf{P} and the output $\hat{\mathbf{P}}$:

$$\hat{\mathbf{P}} = \mathcal{G}_{b2p}\left(\hat{\mathbf{B}},\mathbf{P}\right)$$
 .

The other stream is a binary-to-color network. Given the concatenation of \mathbf{P} as well as the hollow binary volume $\hat{\mathbf{B}}_{ri}$ from $\hat{\mathbf{B}}$, \mathcal{G}_{b2c} generates the RGB volume $\hat{\mathbf{V}}_c$:

$$\hat{\mathbf{V}}_{c}=\mathcal{G}_{b2c}\left(\hat{\mathbf{B}}_{ri},\mathbf{P}
ight)$$
 .

We can obtain the final color volume according to: $\hat{\mathbf{C}} = \hat{\mathbf{V}}_c \odot \mathbf{B}_{ri}$.

3.4. Loss Functions

We use two parts of loss functions to train our whole framework. One part is to train our proposed front-to-back network, and therefore the loss functions are based on the image. The other part, however, is to train our Pose-guided Flowable Networks at the volume level for the human imitation task.

Front-to-back synthesis. To train our front-to-back network, we utilize the functions containing silhouette loss, perceptual loss, pixel-wise Mean Squared Error(MES) loss as well as 2D adversarial loss. Note that we need to train \mathcal{G}_{p2b} and \mathcal{G}_{p2b} with the same loss functions in the task of front-view reconstruction and back-view estimation, respectively. Here we take back-view estimation as an example to show these losses. We use Binary Cross-Entropy(BCE) loss for regularizing the synthesized silhouette with the original one:

$$\mathcal{L}_{sil} = -\frac{1}{|\mathbf{S}_b|} \sum \mathbf{S}_b \cdot \log \mathbf{\hat{S}}_b + (1 - \mathbf{S}_b) \cdot \log \left(1 - \mathbf{\hat{S}}_b\right),$$

where $\hat{\mathbf{S}}_b$ is the synthesized silhouette corresponding to \mathbf{S}_b .

To improve the quality of the synthesized back-view texture, we adopt perceptual loss to regularize $\hat{\mathbf{I}}_b$ to be closer to ground truth \mathbf{I}_b in the learned space of VGG-19 [27]:

$$\mathcal{L}_{p} = \left\| f\left(\hat{\mathbf{I}}_{b}\right) - f\left(\mathbf{I}_{b}\right) \right\|_{1},$$

where $f(\cdot)$ is defined as the pre-trained VGG-19, and $\hat{\mathbf{I}}_{\mathbf{b}}$ is the synthesized version of $\hat{\mathbf{I}}_{\mathbf{b}}$. For pixel-wise regularization, we apply MSE reconstruction loss to preserve the shared visible features that both front and back views own:

$$\mathcal{L}_{pix} = \frac{1}{|\mathbf{I}_b|} \|\hat{\mathbf{I}}_b - \mathbf{I}_b\|_2^2.$$

We, at the same time, train our network in an adversarial manner like PatchGAN to generate clear and sharp back views:

$$\mathcal{L}_{adv} = \sum \mathcal{D} \left(\mathbf{\hat{I}}_b, \mathbf{\hat{S}}_b \right)^2.$$

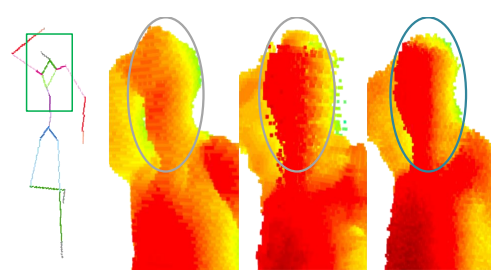


Figure 9. Visual evaluation of our binary head enhancer. From left to right: input pose, refined head, enhanced head, refined head after enhancement.

	SSIM↑	LPIPS↓
PG2	0.891	0.934
LW-GAN	0.912	0.927
Ours	0.903	0.946

Table 1. Quantitive evaluation of our pose-guided flowable networks as compared to most recent methods on THuman dataset. ↑ represents the larger is better, and ↓ means the smaller is better. Note that a higher SSIM may not mean a better quality of image.

Our final objective to train front-to-back translation network is shown as:

$$\mathcal{L}_{sun} = \lambda_p \cdot \mathcal{L}_p + \lambda_{pix} \cdot \mathcal{L}_{pix} + \lambda_{sil} \cdot \mathcal{L}_{sil} + \mathcal{L}_{adv},$$

where we set the relative weights as $\lambda_p = 1.0$, $\lambda_{pix} = \lambda_{pix} = 100.0$ in our experiments.

Human imitation. To train Pose-guided Flowable Networks, we utilize binary-volume loss as well as colored-volume loss corresponding to the two streams shown in Sec. 3.3. We train \mathcal{G}_{p2b} and \mathcal{G}_{b2p} with binary-volume losses, including re-projection silhouette loss. Colored-volume losses to train \mathcal{G}_{b2c} consists of voxel RGB loss, re-projection texture loss as well as volumetric adversarial loss.

To regularize our networks based on occupancy volume, we use weighted BCE loss for reconstruction of ${\bf B}$ as well as ${\bf P}$. The reconstruction error of ${\bf B}$ is shown as:

$$\mathcal{L}_{vox} = -\frac{1}{|\mathbf{B}|} \sum \gamma \mathbf{B} \cdot \log \hat{\mathbf{B}} + (1 - \gamma) (1 - \mathbf{B}) \cdot \log (1 - \hat{\mathbf{B}}),$$

where $\gamma=0.7$, a weight to balance the loss contributions of occupied and unoccupied voxels.

To learn the geometric shape, we adopt re-projection silhouette loss to help to regularize the outline of a volume:

$$\mathcal{L}_{resil} = -\sum_{n} \frac{1}{|\mathbf{S}_{n}|} [\mathbf{S}_{n} \cdot \log \hat{\mathbf{S}}_{n} + (1 - \mathbf{S}_{n}) \cdot \log (1 - \hat{\mathbf{S}}_{n})],$$

where n is the index of viewpoints to render silhouettes. Here we render a front silhouette and a side silhouette given a binary volume. We can obtain a silhouette \mathbf{S}_n by projecting voxels to the 2D plane as follows: $\mathbf{S}_n = g(\mathbf{B}, \theta_n)$, where $g(\cdot)$ is defined as the projecting function, and θ_n is a viewpoint corresponding to the nth face of \mathbf{B} .

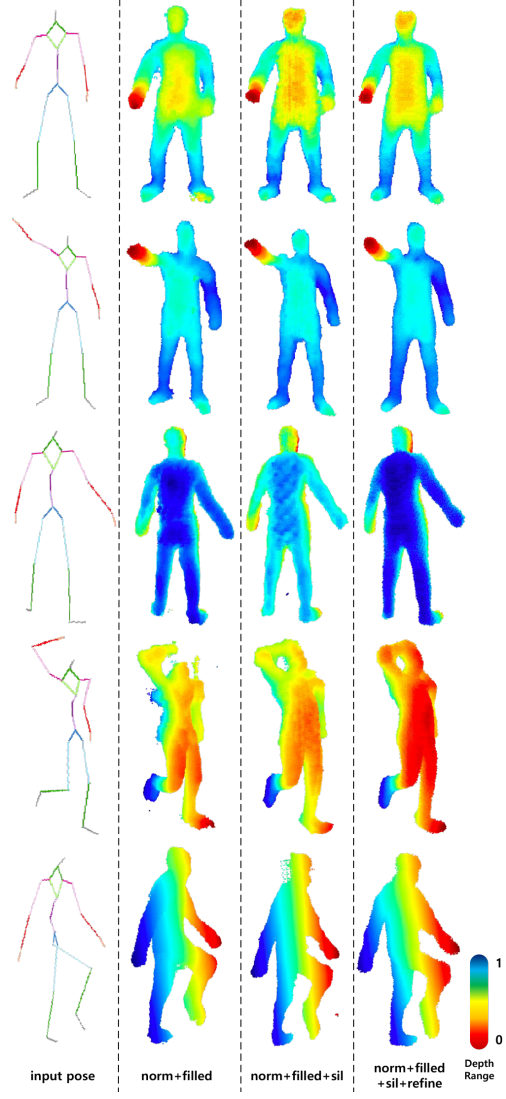


Figure 10. Visual evaluation of our pose-to-binary-volume translation network. From left to right: input pose label, synthesized volume with avatar normalization (norm) and the supervision of filled-in binary volume (filled), synthesized volume with norm, filled and the supervision of differentiable silhouette projector (sil), our final synthesized volumes with norm, filled, sil and a body refiner (refine). A color indicator of depth is shown on the right bottom corner. The depth value decreases from the front (near 0) to the back (near 1).

Similar to image-based PatchGAN, we train our networks with a volume-based PatchGAN to push the distribution of synthesized colored volumes to the distribution of real colored ones:

$$\mathcal{L}_{badv} = \sum \mathcal{D}_b \left(\hat{\mathbf{B}} \right)^2,$$

where \mathcal{D}_b is the discriminator to tell the real binary volume from the fake one. The adversarial loss of colored volume \mathcal{L}_{cadv} is defined similarly.

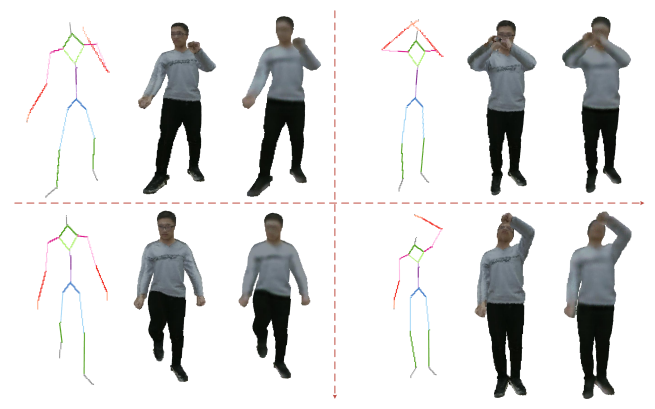


Figure 11. Examples of motion imitation from our proposed methods. From left to right: input pose, ground truth, the generated volumes from our Flowable Networks.

In order to learn a complete texture and to improve its quality, we use a re-projection texture loss, similar to reprojection silhouette loss, to regularize the generated colored volume to be closer to the real one:

$$\mathcal{L}_{retex} = \sum_{m} \frac{\eta_m}{|\mathbf{T}_m|} \|\hat{\mathbf{T}}_n - \mathbf{T}_m\|_1,$$

where m is the index of viewpoints and \mathbf{T}_m represents the rendered RGB image, obtained by: $\mathbf{T}_m = h\left(\mathbf{C}, \theta_m\right)$. Here $h(\cdot)$ is defined as the function to project colored voxel to the 2D plane. The texture weight η_m is to balance the loss contributions of texture \mathbf{T}_m . In our framework, we propose a depth-aware differentiable renderer for volumes, as shown in Fig. 7. Inspired by the depth projector from DeepHuman[35], we render before extracting the surface voxels based on the depth of the volume.

The overall loss functions of binary volume reconstruction and colored volume reconstruction is shown as:

$$\mathcal{L}_{bin} = \lambda_{resil} \cdot \mathcal{L}_{resil} + \lambda_{vox} \cdot \mathcal{L}_{vox} + \mathcal{L}_{badv},$$

$$\mathcal{L}_{color} = \lambda_{retex} \cdot \mathcal{L}_{retex} + \mathcal{L}_{cadv},$$

where we set the relative weights as $\lambda_{pose} = \lambda_{resil} = \lambda_{vox} = 1.0$, $\lambda_{retex} = 3.0$ in our experiment.

4. Experiments

4.1. Implementation

Synthetic dataset. To fit our task better, we have online collected 651 posed meshes with full textures, including 90 from Axyz¹ 83 from Gobotree People², 20 from Render People³ and 458 from 3D People⁴. We split them into a

training set of 418 meshes and a test set of 40 meshes. To render front and back views, we set the projective camera to preserve the original size of body and the original location of each pixel for better projection of voxel. For front-to-back synthesis, we slightly rotate each model in order to render the whole face in the front.

Network architectures. We follow the U-Net network architecture [25] in both the front-to-back translation and the volume-to-volume translation with an input channel size of 4. We apply Xavier initializer [9] to our whole framework. We train our model with stable learning rates of 2.0×10^{-4} and 1.0×10^{-4} at first 40 and 30 iterations and decayed learning rates at another 40 and 30 iterations, respectively. To train our model, we use the Adam optimizer with batch size of 4 and 8. To obtain accurate results, we additionally add 6 and 9 residual blocks following ResNet [11] to the middle of U-Net.

4.2. Results

We demonstrate our approach of texture generation with various human images in Fig. 8. We randomly pick some images rendered from THuman models. As shown in Fig. 8, our approach is able to estimate the back-view texture of the human model within the limitation of front-view silhouette. Our textured volume recovery module allows us to reconstruct the fully textured volumetric body. We additionally exemplify the effectiveness of our human imitation flow in Fig. 11. We randomly sample some volumes with our trained model, driven by a given collection of 3D poses. Our networks trained with only a few posed volumes, are still capable to predict various unseen poses. Thus human imitation flow are capable of generating a sequence of volumes, or volume-based video.

4.3. Comparisons

We evaluate our models with the metrics of Structural Similarity (SSIM) [32] and the LPIPS [34]. Note that prior works of human imitation focus on images and evaluate through image-based metrics. To compare with those methods, we render the frontal images of the generated colored bodies before evaluation.

In Fig. 8., we **qualitatively** compare our front-to-back translation and volume-to-volume translation with SiCloPe front-to-back generator [21].

The **qualitative** comparison against front-to-back rendering in SiCloPe [21] is shown in Fig. 12.

As shown in Tab. 1, to **quantitively** evaluate our poseguided flowable networks, we compare the results with most recent methods, including LW-GAN [17] based on transformation flow and PG2 [19] based on 2D human pose. We train all these methods on THuman dataset, and evaluate through above metrics. Since these methods concentrate on image, we render four views of each human model as the

¹https://secure.axyz-design.com/

²https://www.gobotree.com/

³https://renderpeople.com/

⁴https://3dpeople.com/en/



Figure 12. Comparison of our recovery method with SiCloPe front-to-back rendering. Due to the voxel-level occlusion in a volume, a simple front-to-back rendering cannot handle it. Our proposed penetrable ray plays an important role to solve this problem, shown in Fig. 4

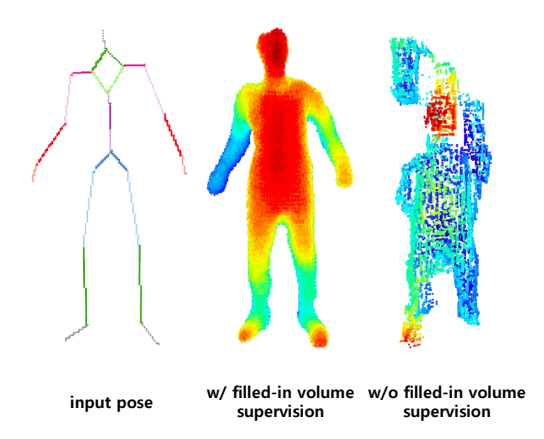


Figure 13. Visual evaluation of choosing which kind of volume as the supervisor in our pose-to-binary-volume translation network. A hollow binary volume cannot be qualified to supervise the network. However, the filled-in volumes fulfill the requirements for training.

training data. We also **qualitatively** compare our human imitation flow with those methods in Tab. 1.

5. Ablation Study

5.1. Front-to-Back Synthesis

To verify the effectiveness of our proposed methods, preflip and silhouette-based attention map, we compare the results with the baseline method, the front-to-back translation network from SiCloPe[21]. The silhouette attention map help limit the outline of the person, while pre-flip convert the front-to-back translation to a more efficient pix-to-pix translation method.

5.2. Pose-to-binary Translation

We compare the results under four different situation, shown in Fig. 10. For the sparsity of the volume, a surface human model like mesh does not work for training. The filled-in volume is the better choice, shown in Fig. 13. With

the assistance of the differentiable silhouette projector, we can train our network efficiently. We additionally add a binary head enhancer and a volume refiner at the end of the network, in order to preserve the geometric information in part and in total respectively.

5.3. Binary-to-color Translation.

As mentioned above, volume is sparse. However, we cannot fill in a colored volume with a specific value. To efficiently train the model and to converge, we propose a depthaware differentiable renderer for supervision. As shown in Fig. 11, it shows its powerful ability to extract 3D features.

6. Conclusion

Limitation. Limitations. Our volume generators are fully relied on volumetric convolution. However, due to the sparsity of a colored volume, volumetric convolution cannot capture the more detailed information. Thus the binary-to-color translation network sometimes generates blurred face or clothing texture. This issue should be addressed in the future. Additionally, the refinement of a binary volume sometimes is over-smoothed and some geometric details are missing. Due to the low-resolution meshes in THuman, the generated volumes are consequently blurred in details as well.

Discussion. We have, for the first time, presented a framework for human recovery as well as imitation from a single image. Given a frontal image, our front-to-back translation network learns to generate the corresponding back image. In order to recover the textured human model, we project both the given front image and the generated back image to the surface of the human volumetric model. We subsequently develop an imitation network, Flowable Networks, for generating human volumetric models guided by 3D poses. We believe our framework will enable convenient VR/AR creation and inspire many researchers to focus on the combination of 3D computer vision and graphics.

References

- [1] Thiemo Alldieck, Gerard Pons-Moll, Christian Theobalt, and Marcus Magnor. Tex2shape: Detailed full human body geometry from a single image. In *Proceedings of the IEEE International Conference on Computer Vision*, pages 2293–2303, 2019. 3
- [2] Rıza Alp Güler, Natalia Neverova, and Iasonas Kokkinos. Densepose: Dense human pose estimation in the wild. In *Proceedings of the IEEE Conference on Computer Vision and Pattern Recognition*, pages 7297–7306, 2018. 2
- [3] Dragomir Anguelov, Praveen Srinivasan, Daphne Koller, Sebastian Thrun, Jim Rodgers, and James Davis. Scape: shape completion and animation of people. In ACM SIGGRAPH 2005 Papers, pages 408–416. 2005. 3
- [4] Guha Balakrishnan, Amy Zhao, Adrian V Dalca, Fredo Durand, and John Guttag. Synthesizing images of humans in unseen poses. In *Proceedings of the IEEE Conference on Computer Vision and Pattern Recognition*, pages 8340–8348, 2018. 2, 4
- [5] Federica Bogo, Angjoo Kanazawa, Christoph Lassner, Peter Gehler, Javier Romero, and Michael J Black. Keep it smpl: Automatic estimation of 3d human pose and shape from a single image. In *European Conference on Computer Vision*, pages 561–578. Springer, 2016. 3
- [6] Caroline Chan, Shiry Ginosar, Tinghui Zhou, and Alexei A Efros. Everybody dance now. In *Proceedings of the IEEE International Conference on Computer Vision*, pages 5933–5942, 2019. 2, 4
- [7] Patrick Esser, Ekaterina Sutter, and Björn Ommer. A variational u-net for conditional appearance and shape generation. In Proceedings of the IEEE Conference on Computer Vision and Pattern Recognition, pages 8857–8866, 2018.
- [8] Valentin Gabeur, Jean-Sébastien Franco, Xavier Martin, Cordelia Schmid, and Gregory Rogez. Moulding humans: Non-parametric 3d human shape estimation from single images. In *Proceedings of the IEEE International Conference on Computer Vision*, pages 2232–2241, 2019. 3
- [9] Xavier Glorot and Yoshua Bengio. Understanding the difficulty of training deep feedforward neural networks. In Proceedings of the thirteenth international conference on artificial intelligence and statistics, pages 249–256, 2010. 7
- [10] Ian Goodfellow, Jean Pouget-Abadie, Mehdi Mirza, Bing Xu, David Warde-Farley, Sherjil Ozair, Aaron Courville, and Yoshua Bengio. Generative adversarial nets. In *Advances* in neural information processing systems, pages 2672–2680, 2014. 2
- [11] Kaiming He, Xiangyu Zhang, Shaoqing Ren, and Jian Sun. Deep residual learning for image recognition. In *Proceedings of the IEEE conference on computer vision and pattern recognition*, pages 770–778, 2016. 7
- [12] Karim Iskakov, Egor Burkov, Victor Lempitsky, and Yury Malkov. Learnable triangulation of human pose. In *Proceedings of the IEEE International Conference on Computer Vision*, pages 7718–7727, 2019. 3
- [13] Phillip Isola, Jun-Yan Zhu, Tinghui Zhou, and Alexei A Efros. Image-to-image translation with conditional adversarial networks. In *Proceedings of the IEEE conference on*

- computer vision and pattern recognition, pages 1125–1134, 2017. 2
- [14] Aaron S Jackson, Chris Manafas, and Georgios Tzimiropoulos. 3d human body reconstruction from a single image via volumetric regression. In *Proceedings of the European Con*ference on Computer Vision (ECCV), pages 0–0, 2018. 3
- [15] Angjoo Kanazawa, Michael J Black, David W Jacobs, and Jitendra Malik. End-to-end recovery of human shape and pose. In *Proceedings of the IEEE Conference on Computer* Vision and Pattern Recognition, pages 7122–7131, 2018. 3
- [16] Christoph Lassner, Javier Romero, Martin Kiefel, Federica Bogo, Michael J Black, and Peter V Gehler. Unite the people: Closing the loop between 3d and 2d human representations. In *Proceedings of the IEEE conference on computer* vision and pattern recognition, pages 6050–6059, 2017. 3
- [17] Wen Liu, Zhixin Piao, Jie Min, Wenhan Luo, Lin Ma, and Shenghua Gao. Liquid warping gan: A unified framework for human motion imitation, appearance transfer and novel view synthesis. In *Proceedings of the IEEE International Conference on Computer Vision*, pages 5904–5913, 2019. 2, 3, 4, 7
- [18] Matthew Loper, Naureen Mahmood, Javier Romero, Gerard Pons-Moll, and Michael J Black. Smpl: A skinned multiperson linear model. ACM transactions on graphics (TOG), 34(6):1–16, 2015. 2, 3
- [19] Liqian Ma, Xu Jia, Qianru Sun, Bernt Schiele, Tinne Tuytelaars, and Luc Van Gool. Pose guided person image generation. In Advances in Neural Information Processing Systems, pages 406–416, 2017. 2, 4, 7
- [20] Liqian Ma, Qianru Sun, Stamatios Georgoulis, Luc Van Gool, Bernt Schiele, and Mario Fritz. Disentangled person image generation. In *Proceedings of the IEEE Con*ference on Computer Vision and Pattern Recognition, pages 99–108, 2018. 2
- [21] Ryota Natsume, Shunsuke Saito, Zeng Huang, Weikai Chen, Chongyang Ma, Hao Li, and Shigeo Morishima. Siclope: Silhouette-based clothed people. In *Proceedings of the IEEE Conference on Computer Vision and Pattern Recognition*, pages 4480–4490, 2019. 2, 3, 4, 5, 7, 8
- [22] Natalia Neverova, Riza Alp Guler, and Iasonas Kokkinos. Dense pose transfer. In *Proceedings of the European conference on computer vision (ECCV)*, pages 123–138, 2018.
- [23] Kyle Olszewski, Sergey Tulyakov, Oliver Woodford, Hao Li, and Linjie Luo. Transformable bottleneck networks. In Proceedings of the IEEE International Conference on Computer Vision, pages 7648–7657, 2019. 4
- [24] Yu Rong, Ziwei Liu, Cheng Li, Kaidi Cao, and Chen Change Loy. Delving deep into hybrid annotations for 3d human recovery in the wild. In *Proceedings of the IEEE International Conference on Computer Vision*, pages 5340–5348, 2019. 3
- [25] Olaf Ronneberger, Philipp Fischer, and Thomas Brox. Unet: Convolutional networks for biomedical image segmentation. In *International Conference on Medical image computing and computer-assisted intervention*, pages 234–241. Springer, 2015. 7

- [26] Chenyang Si, Wei Wang, Liang Wang, and Tieniu Tan. Multistage adversarial losses for pose-based human image synthesis. In *Proceedings of the IEEE Conference on Computer Vision and Pattern Recognition*, pages 118–126, 2018.
- [27] Karen Simonyan and Andrew Zisserman. Very deep convolutional networks for large-scale image recognition. arXiv preprint arXiv:1409.1556, 2014. 5
- [28] Vince Tan, Ignas Budvytis, and Roberto Cipolla. Indirect deep structured learning for 3d human body shape and pose prediction. 2018. 3
- [29] Hsiao-Yu Tung, Hsiao-Wei Tung, Ersin Yumer, and Katerina Fragkiadaki. Self-supervised learning of motion capture. In Advances in Neural Information Processing Systems, pages 5236–5246, 2017. 3
- [30] Gul Varol, Duygu Ceylan, Bryan Russell, Jimei Yang, Ersin Yumer, Ivan Laptev, and Cordelia Schmid. Bodynet: Volumetric inference of 3d human body shapes. In *Proceedings of the European Conference on Computer Vision (ECCV)*, pages 20–36, 2018. 3
- [31] Ting-Chun Wang, Ming-Yu Liu, Jun-Yan Zhu, Andrew Tao, Jan Kautz, and Bryan Catanzaro. High-resolution image synthesis and semantic manipulation with conditional gans. In Proceedings of the IEEE conference on computer vision and pattern recognition, pages 8798–8807, 2018. 2
- [32] Zhou Wang, Alan C Bovik, Hamid R Sheikh, and Eero P Simoncelli. Image quality assessment: from error visibility to structural similarity. *IEEE transactions on image processing*, 13(4):600–612, 2004. 7
- [33] Chung-Yi Weng, Brian Curless, and Ira Kemelmacher-Shlizerman. Photo wake-up: 3d character animation from a single photo. In *Proceedings of the IEEE Conference* on Computer Vision and Pattern Recognition, pages 5908– 5917, 2019. 3
- [34] Richard Zhang, Phillip Isola, Alexei A Efros, Eli Shechtman, and Oliver Wang. The unreasonable effectiveness of deep features as a perceptual metric. In *Proceedings of the IEEE Conference on Computer Vision and Pattern Recognition*, pages 586–595, 2018. 7
- [35] Zerong Zheng, Tao Yu, Yixuan Wei, Qionghai Dai, and Yebin Liu. Deephuman: 3d human reconstruction from a single image. In *Proceedings of the IEEE International Con*ference on Computer Vision, pages 7739–7749, 2019. 2, 3,
- [36] Qian-Yi Zhou, Jaesik Park, and Vladlen Koltun. Open3D: A modern library for 3D data processing. arXiv:1801.09847, 2018. 4